JOURNAL OF COMPLEMENTARY MEDICINE RESEARCH
Journal of Complementary Medicine Research, ISSN: 2146-8397 Vol. 14, No. 1, 2023 (pp.127-132)
RESEARCH ARTICLE
WWW.JOCMR.COM

Influence of Earth Magnetic Field on Animal Nervous System Evolution

Kamila Baba-Ahmed[1*], Béchir Béjaoui[2*], Wafa Feki-Sahnoun[2], Noureddine Mechouk[1], Zihad Bouslama[1,3], Hafedh Abdelmelek[4],

[1]*Terrestrial and Aquatic Systems Ecology Laboratory, Faculty of Sciences, Badji Mokhtar University, BP 12, Annaba, 23005 Sidi Amar, Algeria .*

[2]*Laboratory of Integrated Physiology, Faculty of Sciences, University of Carthage, Jarzouna, Bizerte 7021, Tunisia.*

[3]*National Institute of Science and Technology of the Sea INSTM, 28 rue du 2 mars 1934 Carthage Salambô 2025 Tunis, Tunisia.*

[4]*National Center for Environmental Research, Compus Sidi Amar Annaba 23000, Algéria.*

ABSTRACT

The aim of the present study was to demonstrate the impacts of earth magnetic field (ErMF) on animal nervous system evolution especially electric and histological properties of nerves. We have applied for the first time, as far as we know, a correlation between the influence of ErMF and temperature on superconductor-like behavior in the sciatic nerves of four species. Our question point to answer to the a possible link between magnetic change and climate change and to explain in part the possible implication of both parameters in animal nervous system adaptation and evolution. Our results seem to support the existence of a link between ErMF variation and superconductor-like behavior in nerves. The found link does not mean that the ErMF is fully responsible of the histological, electric properties of nerves and climate changes. The data reveal a decrease in nerve resistivity in chameleon and frog, chick and rabbit; showing a superconductor-like behavior. Analysis of electrical properties demonstrated a clear grade shift at critical temperature (Tc) from poikilotherm (average of ΔT = 11.50) to homeotherm (average of ΔT = 38.00); indicating adaptive nerves changes during evolution confirmed by the increase of Schwann cells number.

Corresponding Author e-mail: kbabaahmed@gmail.com

How to cite this article: Baba-Ahmed K, Béjaoui B, Feki-Sahnoun W, Mechouk N, Bouslama Z, Abdelmelek H (2023) Influence of Earth Magnetic Field on Animal Nervous System Evolution. Journal of Complementary Medicine Research, Vol. 14, No. 1, 2023 (pp. 127-132).

INTRODUCTION

Previous study by Wollin et al. (1971) point that there is a potential link between earth magnetic field (ErMF) and warm climate periods. Bucha (1976) suggested that geomagnetic poles variations could influence atmosphere pressure; leading to sudden climate changes. High values of the solar and/or Earth magnetic field intensity reinforce the shield and then a low density of galactic cosmic rays coming to the solar system and in turn to earth is expected; directly or indirectly probably implicated in animal evolution or extinction (Kitaba et al. 2003, Christl et al. 2004; Snowball et al. 2007; Thoveny et al. 2008, Duplissy et al. 2010; Sato et al. 2013, Wollin et al. 2013). Interestingly, a decreasing in the ErMF intensity would allow a higher entrance of galactic cosmic rays to the earth that could enhance the formation of low-lying clouds leading to tropospheric cooling (Svensmark and Friis-Christensen, 1997; Usoskin, 2008). Moreover, the co-variability of paleomagnetic and paleoclimate time series has been found in many sedimentary records. Most of the reversals of geomagnetic field polarity and magnetic poles' excursions seems to appear in periods of cold climate (Kitaba et al, 2013). This mechanism was invoked to explain the possible relation between the intensity of ErMF and climate on glacial-interglacial timescales, since dipole moment lows seem to occur shortly before the onset of relatively cold intervals. This suggests a connection between low ErMF intensity and climatic cooling. Previous investigations suggested a possible link between centennial-scale cooling episodes and enhanced geomagnetic intensity (Kitaba et al. 2003, Christl et al. 2004, Carrasco et al. 2008; Pavón-Thouveny and Bourlès, 2008; Thouveny et al. 2008, Dergachev et al. 2012). De Santis et al, (2012) proposed three mechanisms to explain this possible link based i) on the entrance of charged particles from space and ii) the possible reduction of the ozone layer and/or iii) a common internal cause shared between both ErMF and Ta time variations (Natalya Andreeva Kilifarska et al, 2022).

Our study aim to investigate the possible adaptation of nerve histology and electric properties by earth magnétique in four species.

KEYWORDS:
Earth Magnetic Field, Globe temperature, Oceans, Climate Change, CO_2 solubility, New York.

ARTICLE HISTORY:
Received : Nov 05, 2022
Accepted : Dec 19, 2022
Published: Jan 08, 2023

DOI:
10.5455/jcmr.2023.14.01.24

MATERIAL AND METHODS

Data Sources and Methodology

The present paper was structured as follows: in the first section, we expose the chosen time series to carry out this analysis between years 1916 and 2016 in the area of (USA). Then, we will study the correlation between ErMF and Ta. In addition, linear regression analysis to determine line equations representing the relationship between earth magnetic field (B tesla), ambient temperature and the year in New York was done. The methodology was based on data harvested from two data 1) ErMF (www.ngdc.noaa.gov) and 2) Ta (http://www.infoclimat.fr/climatologie mensuelle/07156/janvier/1916/New York.html) (USA). The different data of Ta and ErMF in the area were used in order to perform correlation tests; simulation; and graphics.

Statistical Analysis

A simple linear regression analysis to determine line equations representing the relationship between ErMF (B tesla), Ta and the year in New York. Line equations were generated following the form:

$$y = ax + b \text{ (Fox's, 1997).} \quad (1)$$

where y represents the dependent variable (B tesla or temperature), x represents the independent variable (temperature or year), 'a' represents the slope of the regression line, and 'b' represents the y-intercept. The coefficient of determination (R2) was calculated.

Significance of the differences in ErMF (B tesla) and temperature between sampling years was examined through one-way ANOVA tests. This analysis was made for both Ta and ErMF (B tesla).

All the analysis was performed using the R.3.1.1 (R Development Core Team, 2011) package MASS (Venablesand Ripley, 2002).

Animals were euthanized using light anaesthesia. Sciatic nerve samples (n=6) were harvested from chameleon (*Chamaeleo chameleon; 200g*), frogs (*Rana esculenta; 10g*), chick (*Gallus gallusdomesticus; 200g*), and albinos rabbit *(2 Kg)* with light anaesthesia (Halothane 2.50% in air).

The whole experiment was performed in accordance to the code of practice for the care and use of animals for scientific purposes in Faculty of Sciences in (No.201631).

The proximal segments of the sciatic nerves (1cm) were harvested in order to study resistivity and histological study. Sciatic nerves were conserved in Ringer-buffer during 1 to 5 min. Ringer-buffer composition is: $NaHCO_3$ solution at 1%, $CaCl_2$ at 1%, KCl at 1% and NaCl at 0.60%. Then, the electrical resistivity variations of the sciatic nerve with varying temperature were investigated by employing the four-probe technique which is the most common method of determining the critical temperature (Tc) of a superconductor, Tc_{onset} (temperature at which resistivity starts decreasing). In the present experiment, we studied the effect of the decrease and the increase of temperature on nerve resistivity. The temperature variation was achieved using a Helium exchange gas filled cryostat (closed cycle refrigerator). Temperature was measured using a calibrated Si-diode sensor with an accuracy of 0.10 K and was varied from 300K to 200K. Wires are attached to a material via two methods: wires were leaned in chameleon, frog, chick, and rabbit and especially inserted into the nerves of frog. The two external wires (the distance between the 'current' wires: 8 mm) were used as current leads and the other two as the voltage leads (the distance between the 'current' wires: 2 mm) to record potential differences. Through two of these points a voltage is applied, we used a variable current with very low frequency (36Hz). The value of the current used for the resistivity measurements was 20 μA [4, 3] and, if the material is conductive, a current will flow. Then, if any resistance exists in the material, a voltage will appear across the other two points in accordance with Ohm's law. When the material enters a superconductor state, its resistance drops to zero and no voltage appears across the second set of points [4, 3, 5] (Figure. 1).

Tissue Preparation

The animals were sacrificed using light anaesthesia and their sciatic nerves were immediately harvested and fixed in 10% neutral formalin for at least 48 hours; after that, the samples are ready to be placed in a dehydration machine (Leika TP1020).

Dehydration and Lightening

The automatic circulation step was performed using automate. Samples were transferred in different baths of alcohol, toluene and paraffin for 24 hours.

Firstly, the dehydration: This operation aims to take out or extract water from tissues by soaking samples in seven successive baths of alcohol (ethanol) in increasing concentration, one alcohol bath 80°C one hour, three alcohol baths 95°C (1st bath four one hour, 2nd and 3rd bath for one and half hour and three alcohol baths at 100°C.

Secondly, enlightenment through xylene: This will replace or remove alcohol and allow rapid penetration of paraffin into the tissue. Xylene is a solvent that replaces the dehydration agent (alcohol) this step takes place in three successive baths of xylene (1st bath four 2h00, 2nd bath four 2h30 and 3rd bath four 1h30)

The final step of the automatic circulation frequently used two paraffin baths to 57°C to impregnate the samples (1st and 2nd bath four 2h00).

Inclusion

Then the samples are coated in paraffin blocs. The blocks preparation was with paraffin distributor and cold plate (-15°C) which allows the sample orientation. After that, the cutting is carried out according to usual methods using a microtome to a thickness of 3 microns.

Coloration

Four steps : dewaxing by passage through one xylene bath, rehydration by successive passage in alcohol baths at 100°, 90°, 80 ° and water, routine coloration with hematoxylin-eosin (H-E), rapid dehydration by successive passage in alcohol baths at 80°, 90°, 100° and one bath of xylene.

Finally, reading histological sections and images taken with automatic image analyzer microscope (Leica Qwin) [12, 13]

The calculation method of the topography of Schwann cells in different species was performed according to the model showed in figure. 2.

Calculation of Magnetic Values Based on Aurore Equation

The calculation of magnetic values will use Aurore equation (Baba Ahmed et al 2019). The equation describe a link between Ta and magnetic field that allow us to determine the correspondent values of Tco and Tc onset.

Aurore B=p1*T+p2 P1=-6.0142
P2=17420

Statistical Analysis

Statistical analysis of data was performed using analysis of variance (ANOVA) the one-way ANOVA for comparison between two groups. Values were considered statistically significant p below 0.05 and the level of significance indicated as (*) p≤0.01, (**) p≤0.001, (***) p≤0.0001. The data are shown as a mean ± Standard Error of the Mean (SEM).

RESULTS

In chameleon, the R-T curve at 238 K showed a markable decrease in resistivity without reaching the zero point. Leaning the electrical contacts into sciatic nerve showed a stability of the sciatic nerve resistivity at 252 K < T < 300 K and a sudden rise of conductivity were observed below 240 K (Figure. 3). Then, at temperatures lower than 240 K, the resistivity of the nerve remains constant. Secondly, when the electrical contacts were leaned into the frog sciatic nerve, the nerve resistivity decreased slightly with temperature until about 252 K. The nerve resistivity decreased abruptly at temperatures lower than 241 K, to stabilize at a low values (Figure. 1). Moreover, changing the model and conducting probes embedded into the frog sciatic nerve, resulting a linear decrease of the sciatic nerve resistivity is observed for 239 K < T < 300 K and an abrupt rise of conductivity is shown below 235 K. Then, the resistivity of the nerve remains constant and close to one tenth of its ambient temperature value (Figure. 1). Thirdly in chick, the R-T curve at 280 K showed a markedly fall of resistivity without reaching the zero point. We noticed an increase of the sciatic nerve resistivity is observed for 280 K < T < 300 K and an abrupt rise of conductivity were shown below 244 K (Figure. 1). Results from R-T curve at 298 K of rabbit, showed a markedly fall of resistivity without reaching the zero point. Additionally, a decrease of the sciatic nerve resistivity is observed for 258 K < T < 298 K and an abrupt rise of conductivity were shown below 258 K (Figure. 1).

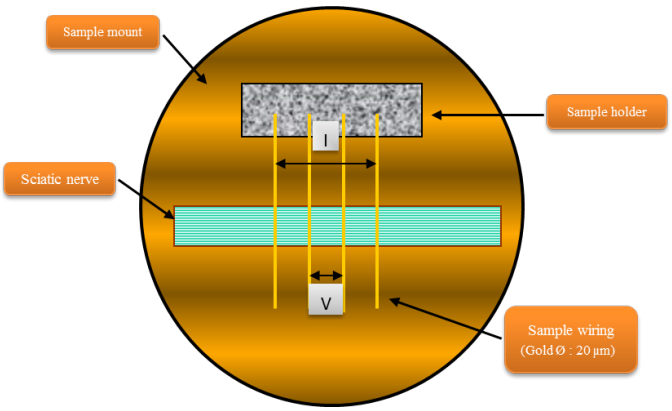

Fig. 1: The Four–point Probe technique (14).

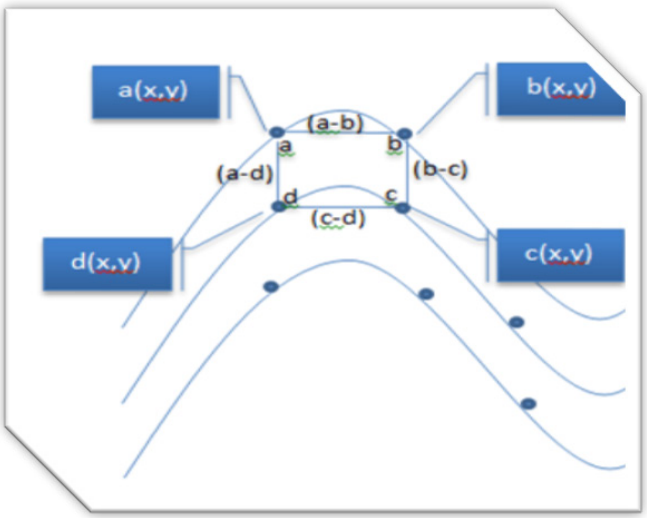

Fig. 2: Calculation methods of the topography of Schwann Cells • ( ) in different species.

The present investigation reported that evolution of species from poikilotherm to homeotherm increases the ΔT average from 11.50 to 38.00 in different nerves in Table 1.

Histological Sections

Longitudinal sections of the sciatic nerves show the presence of nerve fibers with Schwann cells that is surrounding the myelin sheath of chameleon (Figure. 5a), frog (Figure. 5b), chick (Figure. 5c) and rabbit (Figure. 5d).

Evaluation of Schwann n cell number was performed using Image J software. The analysis of the data reported that the most important number of Schwann cells was in homeotherm species compared to poikilotherm (173.50 ± 16.55 vs. 63.75 ± 7.70, ***p=0.0001) (Figure. 6).

The analysis based on the calculation of Schwann cells revealed that during evolution the number and the density increased in the studied species (Figure 7, Figure 8, Figure 9 and Figure 10).

The estimation of the distance a-b, c-d, a-d and b-c demonstrate that these intervals are higher in poikilotherm compared to homeotherm.

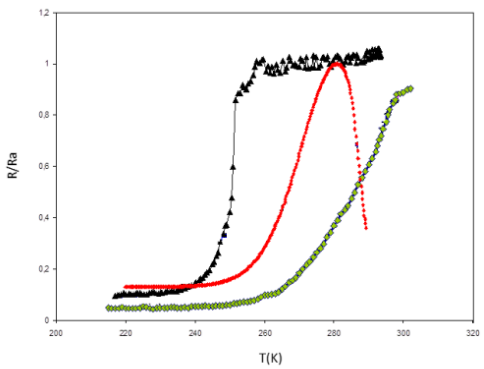

Fig. 3: Comparison of the electrical behavior at low temperature of the sciatic nerves of chameleon (arrows), chick (dotted line), and rabbit .

DISCUSSION

In recent years, several studies have investigated the implication of electrical signals at very low temperature in adaptation of animal species. The study conducted on sciatic nerves of chameleon, frog, chick and rabbit reported remarkable changes in the electrical properties in sciatic nerve of four studied species. However, a prominent decrease in nerve resistivity was observed in (chameleon 252 K), (frog 252 K), (chick 280 K) and (rabbit 298 K); showing a superconductor-like behavior. Analysis of electrical properties demonstrated a clear grade shift at critical temperature (Tc) from poikilotherm to homeotherm; indicating adaptive nerves changes during evolution confirmed by the increase of Schwann cells number as reported in figure 6.

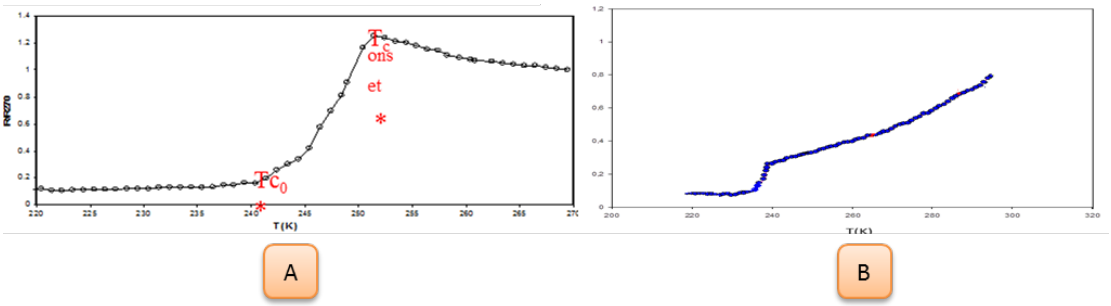

Fig. 4: Evolution of the normalized electric resistance (R/Ra) of the frog sciatic nerve in terms of the temperature T (K) with external recording with the gold past(A), (B) with an internal recording with the gold past (ΔT = 252-241 = 11K).

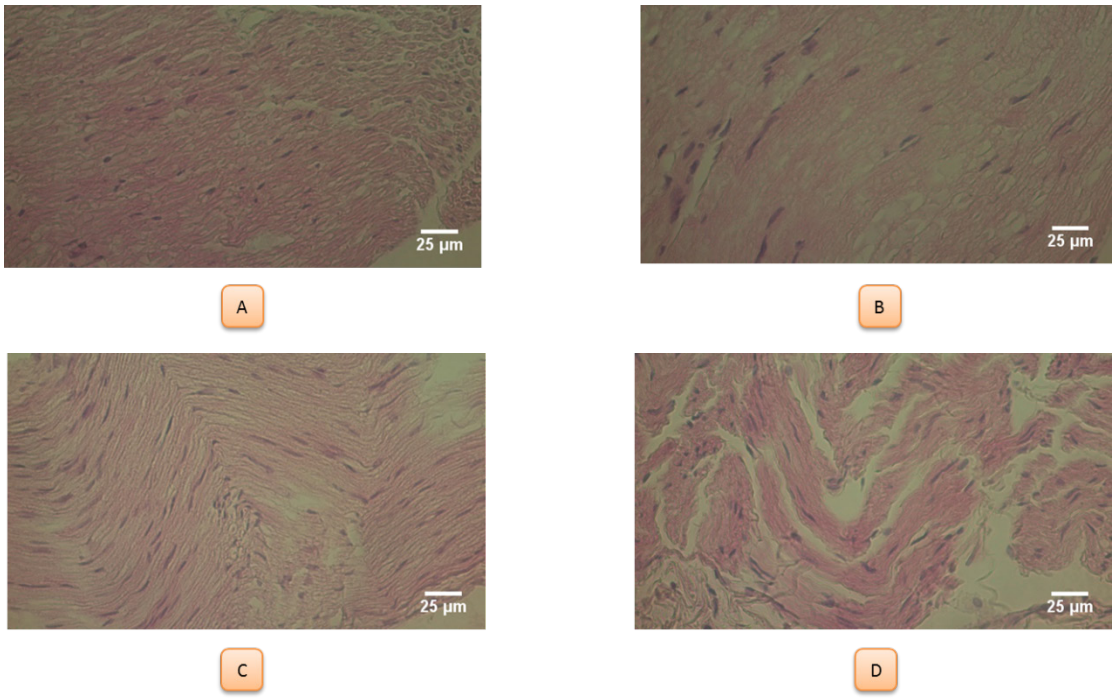

Fig. 5: Longitudinal sections of the sciatic nerve of: (A) chameleon, (B) frog, (C) chick and (D) rabbit. (Hematoxylin-eosin X40)

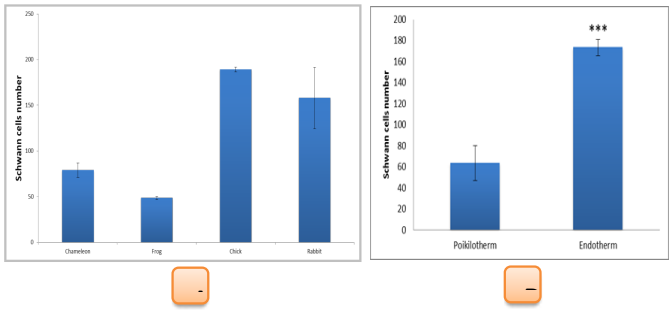

Fig. 6: The number of Schwann cells (A) in four species: chameleon, frog, chick and rabbit (B); in poikilothermvs endotherm. Values are given as the mean ± SEM, for groups of 6 animals each, Schwann cells number of endotherms was compared with poikiloterms ***p=0.0001

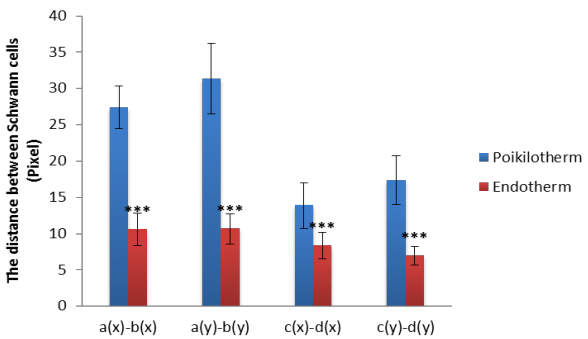

Fig. 7: The distance between two Schwann cells on the same line (point a-b and c-d) in Poikilothermvs Endotherm. Values are given as the mean ± SEM, for groups of six animals each, the distance between Schwann cells of endotherms was compared with poikilotherms ***p=0.0001

As indicated in the methodology, we us Aurore Equation (B=p1*T+p2. (5)) in order to covert Tc on ErMF values during animal evolution. Based on magnetic field and ambient temperature in New York (USA), collected since the beginning of 1916 up to 2016, this data provides not only more evidence for existing coupling between earth magnetic field and climate system, but also offers a bio-physically rational explanation and results supporting its validity related to histological investigation and analysis related to myelin sheaths, Schwann cells ratios.

In view of these results, it would be expected that ErMF decrease could generate a globe temperature increase perhaps implicated in the embedded nerves in endotherm species compared to poikilotherm species as seen by ratio calculation. There are many new theories aiming to explain recent climate changes i) the first of them is that an increase of the ErMF facilitates the entrance of charged particles from space and if the ErMF grows more than it is expected (positive anomaly), then this entrance is favoured; leading to warm atmosphere. Recent works (Bhaskar et al. 2017; Souza et al. 2008) have found interesting correlations between ErMF, solar eruption, and galactic cosmic rays periodic variations and climate change ii) another mechanism proposed a possible reduction of the ozone layer in the upper stratosphere that can cause changes in the climate (Solanki et al. 2013) iii)

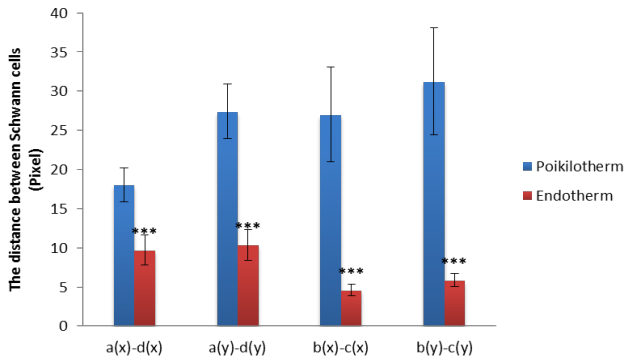

Fig. 9: The distance between two Schwann cells on two superposed lines (point a-d and b-c) in Poikilothermvs Endotherm. Values are given as the mean ± SEM, for groups of 6 animals each, the distance between Schwann cells of endotherms was compared with poikilotherms ***p=0.0001

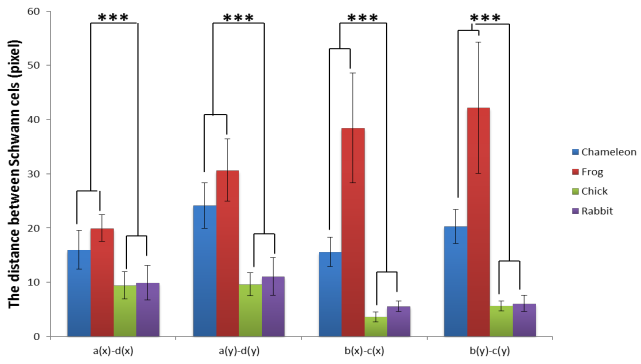

Fig. 8: The distance between two Schwann cells on two superposed lines (point a-d and b-c) in chameleon, frog, chick, and rabbit. Values are given as the mean ± SEM, for groups of 6 animals each, the distance between Schwann cells of endotherms was compared with poikilotherms ***p=0.0001

As we can observe, these two mechanisms relate the solar activity, the galactic cosmic rays production and the ErMF with the Earth's climate, by suggesting that all of them can work together and be needed to complete these mechanism by a new hypothesis implicating the effects of ErMF on Ta variation in different continent in the globe.

In agreement with our results showing ErMF increase and Ta decrease; indicating a negative correlation between both parameters as shown in equation 1. Other studies point out the possible mechanisms that explain these correlations. In the present study, all these works and biophysical mechanisms proposed lead to the deduction that the existence of possible link between the Earth's climate change, the ErMF variation, and animal species adaptation. The co-variability of paleomagnetic and paleoclimate time series has been found in many sedimentary records (Natalya Andreeva Kilifarska et al, 2022). Most of the reversals of geomagnetic field polarity and magnetic poles' excursions seems to appear in periods of cold climate (Kitaba et al, 2013). Data reported that climatic cooling fairly well corresponds to episodes with a stronger geomagnetic field. By contrast, together with objective difficulties for disentangling paleomagnetic from paleoclimate data- due to the high variability and climate dependence of marine sedimentation rates -determines the scepticism of the greater part of scientific community regarding possible links between geomagnetic filed and climate (Natalya Andreeva Kilifarska et al, 2022).

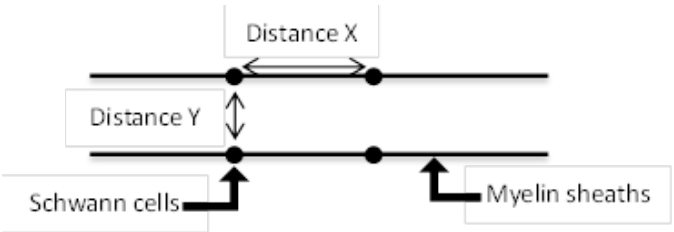

Fig. 10: The model of Schwann cells disposition

Table 1: Transition temperature of the sciatic nerves ofchameleon,frog, chick and rabbit.Values are given as the mean ± SEM, for groups of 6 animals each, ΔT average (K) of endotherms was compared with poikilotherms ***p=0.0001. ***p=0.0001.

		Tc (K)	Tc_{oncet}(K)	Tc0 (K)	ΔT (K)	ΔT average(K)
Chameleon	Leaned	238 ±0.07	252 ±0.09	240 ±0.04	12 ±0.02	Poikilotherms 11.50 ±0.22
Frog	Leaned	238 ±0.05	252± 0.08	241 ±0.09	11 ±0.04	
	inserted	227 ±0.03	239 ±0.02	235 ±0.07		
Chick	Leaned	237 ±0.02	280 ± 0.05	244 ±0.07	36 ± 0.01	Endotherms 38.00 ±0.89***
Rabbit	Leaned	254 ±0.01	298 ±0.08	258±0.06	40±0.03	

Table 2: Calculation of magnetic field using transition temperature of the sciatic nerves of chameleon, frog, chick and rabbit based on Aurore Equation (Baba-Ahmed et al, 2019) .Values are given as the mean ± SEM, for groups of 6 animals each, ΔT average (K) of endotherms was compared with poikilotherms ***p=0.0001. ***p=0.0001.

		CM Tc (nT)	*CM Tconcet(nT)*	*CM Tc0 (nT)*
Chameleon	Leaned	15988.62	15904.42	15976.59
Frog	Leaned	15988.62	15904.42	15970.57
	inserted	16054.77	15982.60	16006.66
Chick	Leaned	15994.63	15736.02	15952.53
Rabbit	leaned	15892.39	15627.68	15868.33

CONCLUSIONS

We have applied for the first time, as far as we know, an analysis of the evolution of ErMF and Ta during hundred years in the New York in order to answer to the question of a possible link between the Earth's magnetic field and climate change and to develop a prediction tools. Our results seem to support the existence of a connection between ErMF variation and Ta anomalies. The found correlation does not mean that the ErMF is fully responsible of the Ta variation and therefore climate changes. Future studies are needed to completely exploit this issue, for example to check other time series at longer timescales and other towns.

Conflict of interest: The authors declare no competing financial interests.

Acknowledgement: the authors are grateful to Bechir AZIB for the technical assistance, providing reagents and equipment.

REFERENCES

1. Abdelmelek, H., Cottet-Emard, J. M., Pequignot, J. M., & Barre, H. (2000). Spinal cord monoaminergic system response to age and cold-acclimatization in Muscovy duckling. *Journal of neural transmission*, *107*(10), 1175-1185.
2. Abdelmelek, H., Chater, S., & Sakly, M. (2001). Acute exposure to magnetic field depresses shivering thermogenesis in rat. 46, 164-166.
3. Abdelmelek, H., Chirgui, M. A., Salem, B. M., & Sakly, M. (2003). Impact of evolution on the electrical properties of sciatic nerves: Superconductivity-like. *Physical and Chemical News http://www. pcnjournal. com/volume _13_ september_2003_088. htm*.
4. Abdelmelek, H., Cottet-Emard, J. M., Pequignot, J. M., & Barré, H. (2003). Sciatic nerve monoaminergic system response to cold acclimatization in Muscovy duckling. *Journal of neural transmission*, *110*(12), 1359-1367.
5. Adam, A., & Friede, R. L. (1988). The number of frog sciatic axons increases continually during body growth. *Anatomy and embryology*, *178*(6), 537-541.
6. Trabelsi, H., Azzouz, I., Ferchichi, S., Tebourbi, O., Sakly, M., & Abdelmelek, H. (2013). Nanotoxicological evaluation of oxidative responses in rat nephrocytes induced by cadmium. *International journal of nanomedicine*, 3447-3453.
7. E.Stålberg, H.Erdem (2000).Nerve conductive studies. NorolBil D, volume 17, issue 2.
8. Ahmed, S., Malik, S., Azeem, M. A., & Noushad, S. (2012). Sciatic nerve conduction velocity and locomotory patterns in Frog, Uromastix and Rabbit. *JAPS, Journal of Animal and Plant Sciences*, *22*(4), 878-883.
9. Lagerspetz, K. Y., & Talo, A. (1967). Temperature Acclimation of the Functional Parameters of the Giant Nerve Fibres in Lumbricus Terrestris L: I. Conduction Velocity and the Duration of the Rising and Falling Phase of Action Potential. *Journal of Experimental Biology*, *47*(3), 471-480.
10. Schön, J. H., Kloc, C., & Batlogg, B. (2000). RETRACTED ARTICLE: Superconductivity in molecular crystals induced by charge injection. *Nature*, *406*(6797), 702-704.
11. Lagerspetz, K. Y., & Talo, A. (1967). Temperature Acclimation of the Functional Parameters of the Giant Nerve Fibres in Lumbricus Terrestris L: I. Conduction Velocity and the Duration of the Rising and Falling Phase of Action Potential. *Journal of Experimental Biology*, *47*(3), 471-480.
12. Barton, R. A., & Harvey, P. H. (2000). Mosaic evolution of brain structure in mammals. *Nature*, *405*(6790), 1055-1058.
13 Waxman, S. G. (1977). Conduction in myelinated, unmyelinated, and demyelinated fibers. *Archives of Neurology*, *34*(10), 585-589.
14. Abdelmelek, H., Hamouda, A. E. M. B., Salem, M. B., Pequignot, J. M., & Sakly, M. (2003). Electrical conduction through nerve and DNA. *Chinese Journal of Physiology*, *46*(3), 137-141.
15. Mbainaibeye, J., Ezzedine, B. B., Mohamed, B. S., Moshen, S., & Abdelmelek, H. (2012). Analysis and characterization of the electrical conductivity behavior of the sciatic nerve using wavelet transform and signal processing. *Int. J. Electron. Commun. Comput. Eng.*, *4*, 2278-4209.
16. Hanini, A., Schmitt, A., Kacem, K., Chau, F., Ammar, S., & Gavard, J. (2011). Evaluation of iron oxide nanoparticle biocompatibility. *International journal of nanomedicine*, *6*, 787.
17. Kasumov, A. Y., Kociak, M., Gueron, S., Reulet, B., Volkov, V. T., Klinov, D. V., & Bouchiat, H. (2001). Proximity-induced superconductivity in DNA. *Science*, *291*(5502), 280-282.
18. Martin, P. M., Cifuentes-Diaz, C., Garcia, M., Goutebroze, L., & Girault, J. A. (2008). Axon and Schwann cells... so far away, so close. *Revue Neurologique*, *164*(12), 1057-1062.